Non-Cooperative Localization and Tracking through the Factorization Method

R. Palmeri, M. T. Bevacqua, A. F. Morabito, and T. Isernia

***Abstract*—The localization and tracking of human targets are cast as linear inverse obstacle problems and solved by means of the Factorization method. The proposed approach is validated against indoor monitoring and multi-frequency sensing, where the Green's function pertaining to the involved realistic scenarios has been determined through full-wave simulations. The results, which include comparisons with the well-known Linear Sampling method as well as the analysis of the impact on final performances of the number of employed transceivers, show a good robustness to noise and model errors.**

***Index Terms*—Microwave imaging, wireless sensor networks.**

I. Introduction

LOCALIZATION and tracking [1] are of high interest in many popular fields including, besides remote sensing, building automation [2] as well as health care and assisted living services [3], and it is also related to the rapid diffusion of wireless sensor networks which are made up of low power consumption devices [4].

Among the very many available localization techniques it is possible distinguishing *cooperative* and *non-cooperative* systems. In the former case, the targets are equipped with a transmitting/receiving tag and actively contribute to the localization process [5]-[7]. However, active systems have some drawbacks related to privacy and cost issues [8]. For this reason, *non-cooperative* systems can represent a good compromise between the deployment costs and the complexity of the detection techniques [8]. As a matter of fact, since targets are device-free, the localization techniques just exploit their interaction with the transmitted signal. In this respect, several approaches have been recently proposed ranging from optical frequencies to radiofrequency and sound waves, and their applicability is clearly related to the specific application at hand [9]-[13].

In such a context, we propose herein a new non-cooperative device-free technique for target tracking and localization in the radiofrequency (RF) regime. In particular, while RF detection techniques are usually based on the analysis of features such as the time of arrival, the direction of arrival, and the received signal's strength or the channel state information [14], in this paper we take advantage of the peculiar feature of the electromagnetic waves to penetrate non-metallic objects and exploit inverse obstacle-based approaches [15]-[17]. These latter, differently from Doppler radar-based approaches [18]-[20], aim at forming an image of the investigated area by evaluating the interaction of the electromagnetic waves with the targets and hence the resulting modification of the propagating waves. More in detail, the scattered field generated by such an interaction is measured by the transceiver nodes, and the electromagnetic properties of targets are then retrieved by solving an inverse scattering problem [21],[22].

Since in a localization problem one only looks for the 'occupancy' detection [1], i.e., for the presence and heads count, it is possible to resort to *qualitative* solution approaches and finally solve a simplified linear problem. In this paper, we pursue such a goal by exploiting the well-known Factorization Method (FM) [23], whose regularized solution provides an energy map and hence a straightforward way to localize the targets. Moreover, we propose the exploitation of the FM at different and consecutive time instants in order to track the changes of position of targets in the considered environment. Finally, a frequency-diversity-based sensing approach is carried out by a proper combination of the FM map indicators in order to further improve localization and tracking (especially when model errors are considered).

The remainder of the paper is organized as it follows. In Section II, the localization problem is cast as an inverse scattering problem. Then, in Section III, the basics of the FM as well as the proposed localization and tracking approach are detailed and discussed. Finally, in Section IV a proof of concept of the introduced method is given for the monitoring of human targets in indoor environments. Conclusions follow.

II. Mathematical Formulation of the Problem

Let us assume, for the sake of simplicity, an invariance of the problem along the *z*-axis and a TM polarization for the electric field. Under the above hypotheses, a 2-D scalar

This is the post-print of the following article: R. Palmeri, M. T. Bevacqua, A. F. Morabito, and T. Isernia, "Non-Cooperative Localization and Tracking through the Factorization Method," IEEE Geoscience and Remote Sensing Letters, vol. 16, n. 8, pp. 1205-1209, 2019. Article has been published in final form at: https://ieeexplore.ieee.org/document/8645656. DOI: 10.1109/LGRS.2019.2895902.

formulation of the inverse scattering problem can be adopted. Let D denote the non-homogeneous investigation domain and $\varepsilon_x(\underline{r}) = \varepsilon_b(\underline{r}) + \Delta\varepsilon(\underline{r})$ its complex permittivity, where $\Delta\varepsilon(\underline{r})$ describes the electromagnetic properties of the targets in D while $\varepsilon_b(\underline{r})$ pertains to the so-called *background scenario*, i.e., to the region of space embedding the targets (see Fig. 1).

In order to detect the targets and retrieve their locations in a known (or a partially-known) scenario, we deal with a *differential* or *distorted* inverse scattering problem [24],[25]. Under such assumptions, and by considering a number N of transmitting/receiving nodes located on a curve Γ, the field ΔE_s scattered from the targets can be expressed as:

$$\Delta E_s(\underline{r}_m, \underline{r}_t) = \int_D G_b(\underline{r}_m, \underline{r}')E(\underline{r}')\Delta\varepsilon(\underline{r}')d\underline{r}' \qquad (1)$$

wherein E is the total field, G_b is the Green's function of the background scenario, and $\underline{r}_m, \underline{r}_t \in \Gamma$ are the locations of the receiving and transmitting nodes, respectively [26]. Finally, the scattered field ΔE_s can be defined as:

$$\Delta E_s(\underline{r}_m, \underline{r}_t) = M(\underline{r}_m, \underline{r}_t) - M_b(\underline{r}_m, \underline{r}_t) \qquad (2)$$

i.e., as the difference between the field $M(\underline{r}_m, \underline{r}_t)$ measured in presence of both the targets and the reference (background) scenario and the field $M_b(\underline{r}_m, \underline{r}_t)$ measured when no targets are present in D [25].

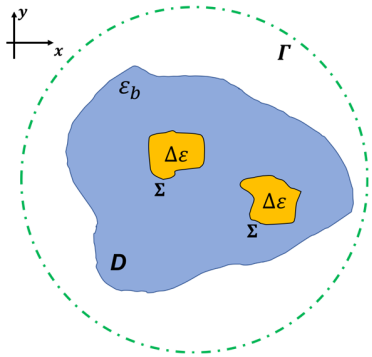

Fig. 1. Sketch of the reference scenario for the mathematical formulation.

The solution of (1) is not a trivial task due to its non-linearity as well as to the ill-posedness [21]. In order to localize and track moving targets, herein we aim at retrieving only their supports and hence, in the following, we adopt *qualitative* solution methods [21],[27],[28]. Among qualitative approaches, the most popular ones are the Linear Sampling method (LSM) [29]-[31] and the FM [23]. In particular, LSM has been widely adopted for detection of unknown targets in several applications, ranging from underground prospecting [30] to through-the-wall imaging [31]. Although very closely related (as both of them belong to the class of *sampling* methods), LSM and FM are different from a mathematical point of view. Indeed, FM allows overcoming some well-known issues arising in LSM [32]. Motivated by this circumstance, in this paper we adopt the FM as a tool to detect and localize targets, as explained in the following Section.

III. Localization and Tracking via Distorted FM

Let us refer to the scenario depicted in Fig. 1, in which one or more targets with cross-section Σ are considered inside the investigation domain D and their location is identified by the coordinates (x_i, y_i). In order to estimate the presence and location of Σ, the FM requires to sample D into a grid of points $\underline{r}_s \in D$ and solve in each of them the following linear equation [23]:

$$\mathcal{F}_m[\xi(\underline{r}_t, \underline{r}_s)] = G_b(\underline{r}_m, \underline{r}_s) \qquad (3)$$

wherein ξ is the actual unknown of the problem and $\mathcal{F}_m = (\mathcal{F}^+\mathcal{F})^{1/4}$ ($\mathcal{F}^+$ being the adjoint of $\mathcal{F}$) is a linear and compact operator whose expression is related to the well-known *far field operator* $\mathcal{F}$ underlying the LSM, which in turn reads [29]:

$$\mathcal{F}: \xi(\underline{r}_t, \underline{r}_s) \rightarrow \int_\Gamma \Delta E_s(\underline{r}_m, \underline{r}_t)\,\xi(\underline{r}_t, \underline{r}_s)d\underline{r}_t \qquad (4)$$

We stress that the basic formulation of the FM by Kirsch et al. [23] is valid for just canonical and homogeneous scenarios, while a distorted formulation [30],[33] is proposed herein.

The evaluation of the weighting coefficients ξ is not straightforward due to the ill-posedness of the problem, so that a regularization technique is required. To this end, the Tikhonov regularization is exploited to achieve a stable solution of (3). In particular, by considering the matrix formulation of the problem (3), its solution can be written as:

$$\boldsymbol{\xi} = \sum_{i=1}^{N} \frac{\sqrt{\lambda_i}}{\lambda_i + \alpha} \langle \boldsymbol{G_b}, u_i \rangle v_i \qquad (5)$$

in which $\boldsymbol{G_b}$ is the vector containing the samples of the background Green's function at the receivers, $(\boldsymbol{u}, \boldsymbol{\lambda}, \boldsymbol{v})$ is the Singular Value Decomposition of the data matrix $\Delta\boldsymbol{E_s}$, and α is the regularization parameter. Interestingly, the energy of the regularized solution $\boldsymbol{\xi}$ keeps bounded for $\underline{r}_s \in \Sigma$, while it is unbounded elsewhere [23]. Therefore, the plot over the sampling grid of the function:

$$\Upsilon(\underline{r}_s) = \sum_{t=1}^{N} \left|\boldsymbol{\xi}(\underline{r}_t, \underline{r}_s)\right|^2 \qquad (6)$$

represents a support indicator for the unknown targets.

It is important to underline that FM allows overcoming some issues arising in LSM. In fact, one possible drawback of LSM is that the corresponding indicator may diverge also for sampling points inside the targets (even in the ideal case of noiseless data) [32]. This drawback is overcome in FM, whose

This is the post-print of the following article: R. Palmeri, M. T. Bevacqua, A. F. Morabito, and T. Isernia, "Non-Cooperative Localization and Tracking through the Factorization Method," IEEE Geoscience and Remote Sensing Letters, vol. 16, n. 8, pp. 1205-1209, 2019. Article has been published in final form at: https://ieeexplore.ieee.org/document/8645656. DOI: 10.1109/LGRS.2019.2895902.

indicator map is more reliable and exhibits a more stable behavior, which is a crucial aspect especially in case of noisy data and model error.

Starting from these circumstances, in the following the FM indicator obtained from (6) is exploited in order to estimate the location coordinates (x_i, y_i) of the targets. More in detail, firstly, a normalized indicator function is defined as [34]:

$$\overline{\Upsilon}(\underline{r}_s) = \frac{\log_{10}(\Upsilon) - \log_{10}(\Upsilon_{max})}{(\log_{10}(\Upsilon) - \log_{10}(\Upsilon_{max}))_{min}} \quad (7)$$

where the subscripts *max* and *min* indicate the maximum and minimum values, respectively. Then, in order to discern between points inside and outside the targets and, so, to estimate the number of targets, a binary mask $\Pi(\underline{r}_s)$ is introduced by fixing a threshold $Th \in (0,1)$. From a mathematical point of view, $\Pi(\underline{r}_s)$ can be expressed as:

$$\Pi(\underline{r}_s) = \begin{cases} 1 & \forall \underline{r}_s : \overline{\Upsilon}(\underline{r}_s) \geq Th \\ 0 & elsewhere \end{cases} \quad (8)$$

Finally, the acquisition of the central coordinates (x_i, y_i) of each non-null area is performed.

In order to improve the resolution of the achieved map, it is possible to exploit a multi-frequency sensing procedure. In particular, by denoting with F the number of exploited frequencies, a multi-frequency indicator can be defined as:

$$\Upsilon_{MF}(\underline{r}_s) = \frac{1}{N_F} \sum_{j=1}^{F} \frac{\Upsilon_j}{\Upsilon_{j,max}} \quad (9)$$

(see also [30]) and then normalized as in equation (7).

The overall procedure can be also exploited for the tracking of moving targets. In fact, by simply solving a set of localization problems at successive time instants, one is able to monitor the targets' movements. In particular, by denoting with K the number of recorded frames, the approach consists in processing $\Delta E_s^{(t_k)}(\underline{r}_m, \underline{r}_t) = M^{(t_k)}(\underline{r}_m, \underline{r}_t) - M_b(\underline{r}_m, \underline{r}_t)$, $\forall k = 1, \ldots, K$, as explained in the following Section.

IV. Numerical Assessment

In order to assess its capabilities in a scenario of actual interest, according to some recent contributions published on these Letters [19],[20], the localization and tracking of human targets in realistic indoor environments have been considered, as detailed in the following.

A realistic indoor environment has been defined (see Fig. 2) where a square ($4m \times 4m$ large) room has been considered filled up by air ($\varepsilon_b = 1$) and surrounded by concrete walls $20cm$ thick ($\varepsilon = 8, \sigma = 10^{-3} S/m$, σ being the conductivity). Inside the room, a plastic chair $30cm \times 20cm$ large ($\varepsilon = 2.5, \sigma = 0$) and a $30cm \times 80cm$ wooden table ($\varepsilon = 3, \sigma = 0$) have also been considered, and N nodes (with $\underline{r}_m = \underline{r}_t$) have been located on the walls in such a way that Γ coincides with the room's inner perimeter.

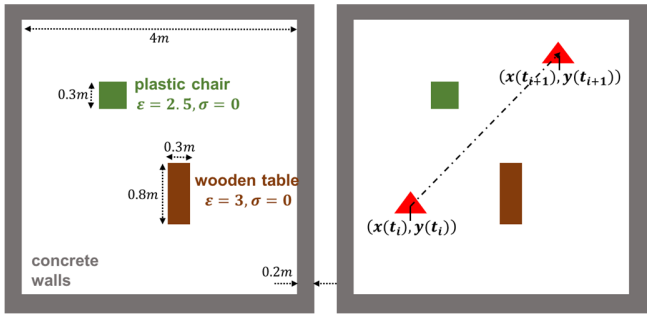

Fig. 2. Reference scenario (red triangles representing the moving target).

In order to ensure the maximum reliability of results, the Green's function G_b pertaining to the background has been computed through full-wave simulations through the COMSOL Multiphysics© package based on the finite-element method. Accordingly, G_b has been computed as the total field present in the room when human targets are not present, while M_b has been set as the field evaluated at the nodes' positions.

In order to realistically mimic a human body, the target has been modeled with the electrical properties of muscles ($\varepsilon = 56.44, \sigma = 0.82\, S/m$), as suggested by [35], and its cross-section has been considered $40cm \times 20cm$ large. The simulated data M have been evaluated at the same positions as those pertaining to M_b, and ΔE_s has been computed according to (2) and then corrupted with a white Gaussian noise with a given signal-to-noise ratio (SNR).

The accuracy of the proposed localization and tracking approach has been evaluated by defining the 'synthetic' error:

$$err_{loc} = \frac{\sqrt{(x - \tilde{x})^2 + (y - \tilde{y})^2}}{\sqrt{x^2 + y^2}} \quad (10)$$

(x, y) and $(\tilde{x}, \tilde{y})$ being the actual and retrieved coordinates identifying the positions of the human targets, respectively.

As a first test case, we dealt with the localization of one person positioned at $(x = -0.65, y = -0.6)m$. By considering a sampling grid of 78×78 square cells, the FM equation (3) has been solved and the indicator function $\overline{\Upsilon}$ has been computed. The achieved results are shown in Fig. 3. As it can be seen, in the case of N=32 the presence of the target has been clearly detected, despite the high amount of noise. Then, the location of the detected target has been retrieved by defining the binary mask Π ($Th = 0.8$) and picking up the central position, as shown in figures 3(b) and 3(d). The corresponding location error is 0.015. For the sake of comparison, Fig. 3 also shows the results obtained when LSM

This is the post-print of the following article: R. Palmeri, M. T. Bevacqua, A. F. Morabito, and T. Isernia, "Non-Cooperative Localization and Tracking through the Factorization Method," IEEE Geoscience and Remote Sensing Letters, vol. 16, n. 8, pp. 1205-1209, 2019. Article has been published in final form at: https://ieeexplore.ieee.org/document/8645656. DOI: 10.1109/LGRS.2019.2895902.

is used instead of FM. As it can be seen, the two approaches are equivalent in term of performances, as both are able to accurately detect and localize the target.

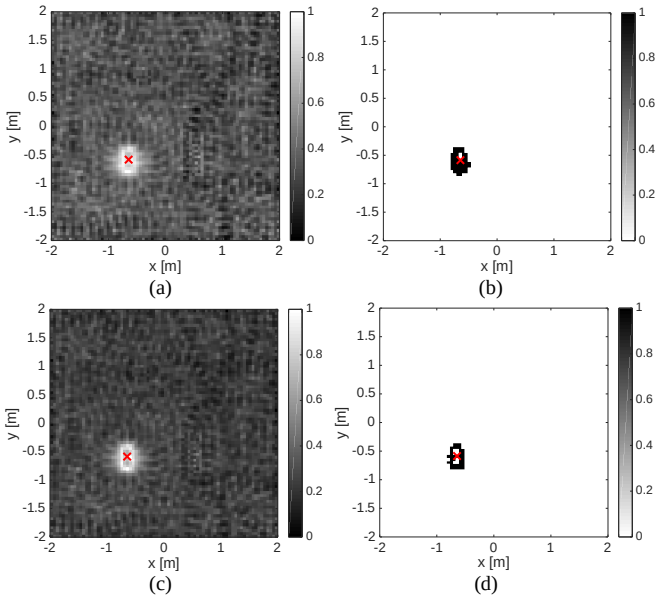

Fig. 3. First test case: Localization step. FM Indicator maps (a) and masks (b) in case of N=32 SNR=15dB. Subplots (c)-(d): the same as (a)-(b) but for LSM indicator and mask. The red cross indicates the retrieved position.

In order to evaluate the impact on performances of the number and location of nodes, Fig. 4 shows a comparison of the indicator maps for SNR=15dB and N=16 in case of equally-spaced and randomly-spaced nodes. Notably, in both cases the detection and the localization of the target have been successfully performed (err_{loc} = 0.015).

A further analysis has been carried out to test the robustness against model errors. In fact, up to now we have supposed to exactly know the interior design of the room. However, any change in it could affect the Green's function G_b in (3). To take into account this circumstance, we solved (3) by considering an inexact version of G_b by adding a high level of white Gaussian noise (SNR=5dB).

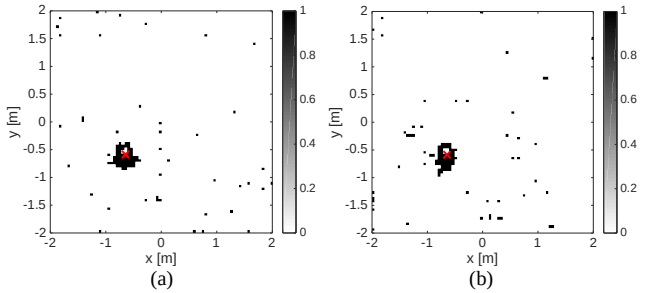

Fig. 4. First test case: Localization step and variation of the number and location of nodes. Retrieved masks for SNR=15dB in case of N=16 and equally-spaced (a) and randomly-spaced (b) nodes.

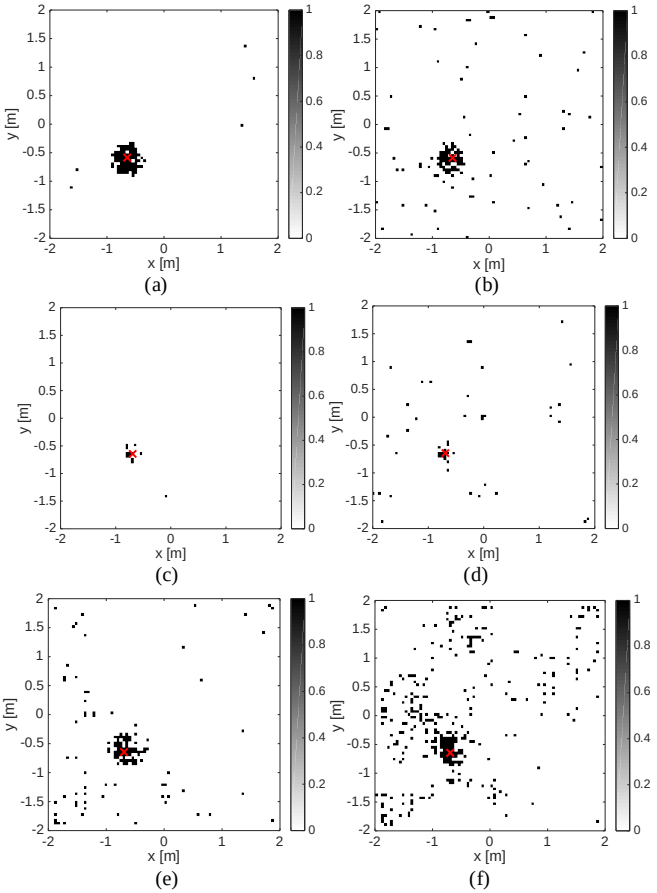

Fig. 5. First test case: localization step and robustness analysis with respect to model error. Retrieved masks (Th = 0.75) for SNR=30dB with N=32 (left) and SNR=15dB with N=24 randomly spaced nodes (right), in case of: inexact Green's function (top) ($err_{loc}^{30dB} = err_{loc}^{15dB}$ = 0.02), Green's function pertaining to an empty room (center) (err_{loc}^{30dB} = 0.1, err_{loc}^{15dB} = 0.15), and Green's function pertaining to an empty room in conjunction with frequency diversity data processing (bottom) ($err_{loc}^{30dB} = err_{loc}^{15dB}$ = 0.06).

In figures 5(a) and 5(b) the localization results are shown in case of inexact G_b with SNR=30dB and SNR=15dB, while figures 5(c) and 5(d) report the results obtained by considering the Green's function pertaining to an empty room, i.e., by completely neglecting the presence of the chair and the table. As it can be seen, the FM-based localization method resulted robust with respect to the model error even in case of noisy data and a reduced number of nodes. Obviously, the more cumbersome backgrounds are considered, the higher the model error may result. Interestingly, in such cases, in order to compensate the higher model error, the localization results can be improved by exploiting the multi-frequency indicator (8) as shown in figures 5(e) and 5(f). In particular, in such an experiment a frequency range from 1GHz to 2GHz (with a step of 250MHz) has been considered.

Besides localization, a sequence in time of FM solutions allowed tracking the target's movements. In this respect, in

This is the post-print of the following article: R. Palmeri, M. T. Bevacqua, A. F. Morabito, and T. Isernia, "Non-Cooperative Localization and Tracking through the Factorization Method," IEEE Geoscience and Remote Sensing Letters, vol. 16, n. 8, pp. 1205-1209, 2019. Article has been published in final form at: https://ieeexplore.ieee.org/document/8645656. DOI: 10.1109/LGRS.2019.2895902.

Fig. 6 the tracking of the target is reported for K=5 time instants and N=24 randomly distributed nodes. Moreover, a comparison between SNR=30dB and SNR=15dB is provided, confirming both the accuracy and robustness of the method.

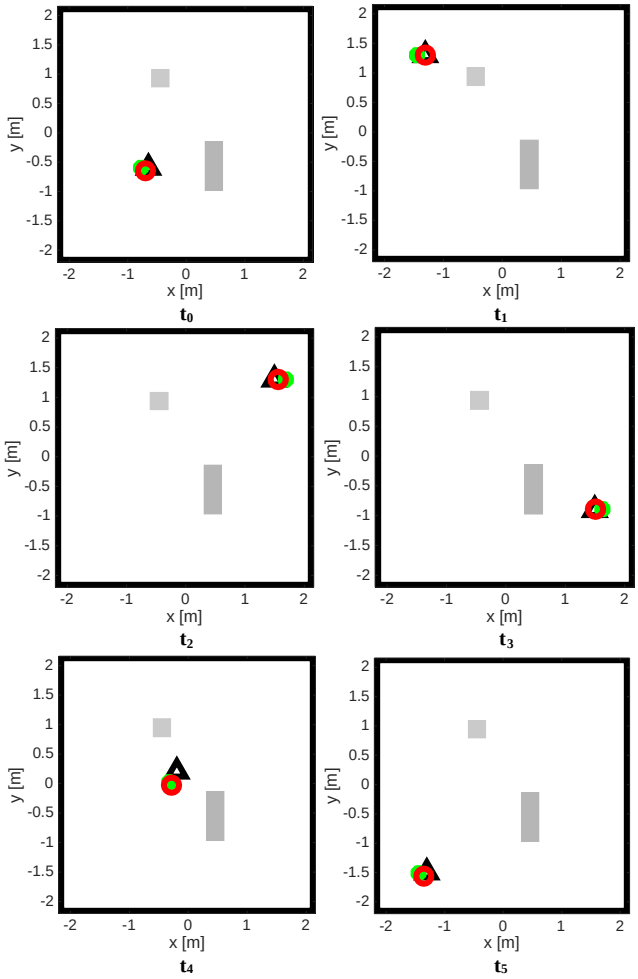

Fig. 6. First test case: Tracking step. The black triangles represent the actual position, while the red and green markers are the estimated positions for SNR=30dB ($err_{loc}^{t_0}$ = 0.14, $err_{loc}^{t_1}$ = 0.08, $err_{loc}^{t_2}$ = 0.09, $err_{loc}^{t_3}$ = 0.07, $err_{loc}^{t_4}$ = 0.64, $err_{loc}^{t_5}$ = 0.07) and SNR=15dB ($err_{loc}^{t_0}$ = 0.06, $err_{loc}^{t_1}$ = 0.006, $err_{loc}^{t_2}$ = 0.032, $err_{loc}^{t_3}$ = 0.007, $err_{loc}^{t_4}$ = 0.80, $err_{loc}^{t_5}$ = 0.04), respectively, in case of inexact Green's function (SNR=5dB) and N=24.

The second test case concerns the localization and tracking of two individuals initially located at $(x = -0.65, y = -0.6)m$ and $(x = 1.31, y = -1.3)m$, respectively. The corresponding synthetic errors are listed in Tab. 1, where a comparison of performances by considering the model error and a reduction in the number of nodes is reported. The involved experiments have been also performed via LSM instead of FM, leading to the same performances. For the sake of brevity, these results are not shown.

Target	Time instant	Exact G_b N=32	Inexact G_b (SNR=5dB),N=32	inexact G_b (SNR=5dB),N=24
#1	t_0	0.015	0.006	0.067
	t_1	0.047	0.006	0.061
	t_2	0.07	0.006	0.067
#2	t_0	0.006	0.023	0.014
	t_1	0.006	0.042	0.049
	t_2	0.024	0.023	0.033

Tab. 1. Second test case: localization errors for the two targets, SNR=15dB.

V. Conclusions

A new approach has been proposed for multi-object localization and tracking by jointly exploiting the inverse scattering paradigm, the distorted Factorization method, and a multi-frequency strategy.

The technique has been assessed against the human targets localization and tracking in realistic indoor environments. The outcomes, which included comparisons with the well-known Linear Sampling method as well as investigations on the impact of the number of employed transceivers, have proved a good robustness to both noise on data and model errors.

Acknowledgment

The authors thank Prof. Sorbello (Università di Catania) for having supported the full-wave experiments.

References

[1] S. Palipana, B. Pietropaoli, and D. Pesch, "Recent advances in RF-based passive device-free localization for indoor applications," *Ad Hoc Networks*, vol. 64, pp. 80-98, 2017.

[2] Wilson, J., and N. Patwari, "See through walls: Motion tracking using variance-based radio tomography networks," *IEEE Trans. Mobile Comput.*, vol. 10, n. 5, pp. 612–621, 2010.

[3] H. Wang, D. Zhang, Y. Wang, J. Ma, Y. Wang, and S. Li, "RT-fall: a real-time and contactless fall detection system with commodity WiFi devices," *IEEE Trans. Mobile Comput.*, vol. 16, n. 2, pp. 511–526, 2017.

[4] J. Yick, B. Mukherjee, and D. Ghosal, "Wireless sensor network survey," *Computer Networks*, vol. 52, n. 12, pp. 2292–2330, 2008.

[5] X. Li, "Collaborative localization with received-signal-strength in wireless sensor networks," *IEEE Trans. Veh. Technol.*, vol. 56, n. 6, pp. 3807–3817, 2007.

[6] A. B. M. Musa and J. Eriksson, "Tracking Unmodified Smartphones Using Wi-Fi Monitors," *Sensor Systems*, pp. 281–294, 2012.

[7] N. Li, G. Calis, and B. Becerik-Gerber, "Measuring and monitoring occupancy with an RFID based system for demand-driven HVAC operations," *Automation in Construction*, vol. 24, pp. 89–99, 2012.

[8] Youssef, Moustafa, Matthew Mah, and Ashok Agrawala, "Challenges: device-free passive localization for wireless environments," *13th Annual International Conf. on Mobile Computing and Networking*, Montréal, Canada, September 9-14, 2007.

[9] R. M. Buehrer, C. R. Anderson, R. K. Martin, N. Patwari, and M. G. Rabbat, "Introduction to the special issue on non-cooperative localization networks," *IEEE J. Sel. Topics Signal Process.*, vol. 8, n. 1, pp. 2–4, 2014.

[10] M. Moussa and M. Youssef, "Smart devices for smart environments: Device-free passive detection in real environments," *IEEE International Conf. on Pervasive Computing and Communications*, 1–6, Galveston, Texas, 9-13 March 2009.

This is the post-print of the following article: R. Palmeri, M. T. Bevacqua, A. F. Morabito, and T. Isernia, "Non-Cooperative Localization and Tracking through the Factorization Method," IEEE Geoscience and Remote Sensing Letters, vol. 16, n. 8, pp. 1205-1209, 2019. Article has been published in final form at: https://ieeexplore.ieee.org/document/8645656. DOI: 10.1109/LGRS.2019.2895902.

[11] N. Patwari and J. Wilson, "RF sensor networks for device-free localization: Measurements, models, and algorithms," *Proc. of the IEEE*, vol. 98, n. 11, pp. 1961-1973, 2010.
[12] J. Jia, M. Liu, and X. Li, "Acoustic passive localization algorithm based on wireless sensor networks," *IEEE International Conf. on Mechatronics and Automation*, pp. 1145-1149, 9-12 Aug 2009, Changchun, China.
[13] B. Song, H. Choi, and H. S. Lee, "Surveillance tracking system using passive infrared motion sensors in wireless sensor network," *International Conf. on Information Networking*, 23-25 Jan. 2008, Busan, Korea.
[14] F. Viani, P. Rocca, G. Oliveri, D. Trinchero, and A. Massa, "Localization, tracking, and imaging of targets in wireless sensor networks: an invited review," *Radio Sci.*, vol. 46, n. 5, pp. 1-12, 2011.
[15] J. Wilson and N. Patwari, "Radio tomographic imaging with wireless networks," *IEEE Trans. Mobile Comput.*, vol. 9, n. 5, pp. 621–632, 2010.
[16] J. Wilson and N. Patwari, "See through walls: motion tracking using variance-based radio tomography networks," *IEEE Trans. Mobile Comput.*, vol. 10, n. 5, pp. 612–621, 2010.
[17] F. Viani, P. Rocca, M. Benedetti, G. Oliveri, and A. Massa, "Electromagnetic passive localization and tracking of moving targets in a WSN-infrastructured environment," *Inv. Prob.*, vol. 26, n. 7, pp. 1-15, 2010.
[18] K. Youngwook and S. S. Sekhon, "Detection of moving target and localization of clutter using Doppler radar on mobile platform," *IEEE Geosci. Remote Sens. Lett.*, vol. 12, n. 5, pp. 1156-1160, 2015.
[19] Y. Ding, X. Lin, K. Sun, X. Xu, and X. Liu, X, Human target localization using Hough transform and Doppler processing, *IEEE Geosci. Remote Sens. Lett.*, vol. 13, n. 10, pp. 1457-1461, 2016.
[20] X. Lin, Y. Ding, X. Xu, and K. Sun, "Human target localization algorithm using energy operator and Doppler processing," *IEEE Geosci. Remote Sens. Lett.*, vol. 15, n. 4, pp. 517-521, 2018.
[21] D. Colton, and R. Kress, "Inverse Acoustic and Electromagnetic Scattering Theory," *Springer-Verlag*, Berlin, Germany, 1992.
[22] M. D'Urso, T. Isernia, and A. F. Morabito, "On the solution of 2-D inverse scattering problems via source-type integral equations," *IEEE Trans. Geosci. Remote Sens.*, vol. 48, n. 3, pp. 1186-1198, 2010.
[23] A. Kirsch, N. I. Grinberg, "The Factorization Method for Inverse Problems," *Cambridge*, 2008.
[24] M. T. Bevacqua and R. Scapaticci, "A compressive sensing approach for 3D breast cancer microwave imaging with magnetic nanoparticles as contrast agent," *IEEE Trans. Med. Imag.*, vol. 35, n. 2, pp. 665-673, 2016.
[25] L. Di Donato, R. Palmeri, G. Sorbello, T. Isernia, and L. Crocco, "A new linear distorted-wave inversion method for microwave imaging via virtual experiments," *IEEE Trans. Microw. Theory Tech.*, vol. 64, n. 8, pp. 2478-2488, 2016.
[26] O. M. Bucci and T. Isernia, "Electromagnetic inverse scattering: retrievable information and measurement strategies," *Radio Sci.*, vol. 32, n. 6, pp. 2123-2137, 1997.
[27] M. Bevacqua and T. Isernia, "Shape Reconstruction via Equivalence Principles, Constrained Inverse Source Problems and Sparsity Promotion," *Progress In Electromagnetics Research*, 158: 37-48, 2017.
[28] M. T. Bevacqua and T. Isernia, "Boundary Indicator for Aspect Limited Sensing of Hidden Dielectric Objects," *IEEE Geosci. Remote Sens. Letters*, vol. 15, n. 6, pp. 838-842, 2018.
[29] D. Colton, H. Haddar, and M. Piana, "The linear sampling method in inverse electromagnetic scattering theory," *Inv. Prob.*, vol. 19, n. 6, pp. 105-137, 2003.
[30] I. Catapano, L. Crocco and T. Isernia, "Improved Sampling Methods for Shape Reconstruction of 3-D Buried Targets," *IEEE Trans. Geosci. Remote Sens*, vol. 46, n. 10, pp. 3265-3273, 2008.
[31] I. Catapano and L. Crocco, "A Qualitative Inverse Scattering Method for Through-the-Wall Imaging," *IEEE Geosci. Remote Sens. Letters*, vol. 7, n. 4, pp. 685-689, Oct. 2010.
[32] L. Crocco, L. Di Donato, I. Catapano, and T. Isernia, "The Factorization Method for Virtual Experiments Based Quantitative Inverse Scattering," *Progress In Electromagnetics Research*, 157: 121-131, 2016.
[33] M. N. Akıncı, T. Çağlayan, S. Özgür, U. Alkaşı, M. Abbak, and M. Çayören, "Experimental Assessment of Linear Sampling and Factorization Methods for Microwave Imaging of Concealed Targets," *International Journal of Antennas and Propagation*, vol. 2015, 2015.
[34] L. Di Donato, M. T. Bevacqua, L. Crocco, and T. Isernia, "Inverse scattering via virtual experiments and contrast source regularization," *IEEE Trans. Antennas Propag.*, vol. 63, n. 4, pp. 1669-1677, 2015.
[35] Y. Suzuki, M. Baba, M. Taki, K. Fukunaga, and S. Watanabe, "Imaging the 3D temperature distributions caused by exposure of dielectric phantoms to high-frequency electromagnetic fields," *IEEE Trans. Dielectr. Electr. Insul.*, vol. 13, n. 4, pp. 744-750, 2006.

This is the post-print of the following article: R. Palmeri, M. T. Bevacqua, A. F. Morabito, and T. Isernia, "Non-Cooperative Localization and Tracking through the Factorization Method," IEEE Geoscience and Remote Sensing Letters, vol. 16, n. 8, pp. 1205-1209, 2019. Article has been published in final form at: https://ieeexplore.ieee.org/document/8645656. DOI: 10.1109/LGRS.2019.2895902.